ISET Journal of Earthquake Technology, Paper No. 481, Vol. 44, No. 1, March 2007, pp. 169–192

A RESPONSE SPECTRUM-BASED NONLINEAR ASSESSMENT TOOL FOR PRACTICE: INCREMENTAL RESPONSE SPECTRUM ANALYSIS (IRSA)

M. Nuray Aydınoğlu
Department of Earthquake Engineering
Kandilli Observatory and Earthquake Research Institute (KOERI)
Boğaziçi University, Istanbul, Turkey

ABSTRACT

Response Spectrum Analysis (RSA) procedure has become a standard analysis tool in traditional strength-based design of buildings and bridges under reduced seismic loads. RSA has been recently extended to estimate nonlinear seismic demands. The Incremental Response Spectrum Analysis (IRSA) procedure is based on a straightforward implementation of RSA at each piecewise linear incremental step in between the formation of consecutive plastic hinges. The practical version of IRSA works directly with smoothed elastic response spectrum and makes use of the well-known "equal displacement rule" to scale modal displacement increments at each piecewise linear step. IRSA can be characterized as an adaptive multi-mode pushover procedure, in which modal pushover analyses are simultaneously performed for each mode at each incremental step under appropriately scaled modal displacements followed by an application of a modal combination rule. Examples are given to demonstrate the practical implementation of IRSA.

KEYWORDS: Incremental Response Spectrum Analysis, Multi-mode Pushover Analysis, Performance-Based Assessment and Design, Inelastic Spectral Displacement, Equal Displacement Rule

INTRODUCTION

The "Response Spectrum Analysis" (RSA) procedure has become a standard design tool in analysis of buildings and bridges under reduced seismic loads. In spite of the approximate nature of modal combination rules involved, multi-mode RSA has proven to be a powerful and easy-to-use method with a rational representation of modal dynamic properties as well as the direct definition of the seismic input through design response spectrum. Today RSA has been incorporated in a standard fashion in almost all modern seismic design codes as part of the "strength-based seismic design" process and it provides a reasonably accurate estimation of the peak seismic demand quantities in the linear range.

On the other hand, during the course of progress of earthquake engineering in the last few decades researchers and engineers have become well aware that structural behavior and eventual damageability of structures during strong earthquakes were essentially controlled by the inelastic deformation capacities of the ductile structural elements. Accordingly, it has been concluded that the seismic evaluation and design of structures should be based on nonlinear deformation demands, not on linear stresses induced by reduced seismic forces that crudely correlated with an "assumed" overall ductility capacity of a given type of a structure. Consequently, the last decade has witnessed the advent of the "performance-based design" concept, in which significant progress has been achieved with the development of "practice-oriented nonlinear analysis procedures" based on the so-called "pushover analysis".

All pushover analysis procedures can be considered as approximate extensions of the response spectrum method to the nonlinear response analysis with varying degrees of sophistication. For example, "Nonlinear Static Procedure—NSP" (ATC, 1996; FEMA, 2000) may be looked upon as a "single-mode inelastic response spectrum analysis" procedure where the peak response is obtained through a nonlinear analysis of a modal single-degree-of-freedom (SDOF) system. In practical applications, modal peak response can be appropriately estimated through "inelastic displacement spectrum" (FEMA, 2000; CEN, 2003).

Note that single-mode pushover analysis can be reliably applied to only two-dimensional response of low-rise building structures regular in plan or simple regular bridges, where the seismic response is essentially governed by the fundamental mode. There is no doubt that application of single-mode pushover to high-rise buildings or any building irregular in plan as well as to irregular bridges involving three-dimensional response would lead to incorrect, unreliable results. Therefore, a number of improved pushover analysis procedures have been offered in recent years in an attempt to take higher mode effects into account (Gupta and Kunnath, 2000; Elnashai, 2002; Antoniou et al., 2002; Chopra and Goel, 2002; Kalkan and Kunnath, 2004; Antoniou and Pinho, 2004a, 2004b). In this context, "Incremental Response Spectrum Analysis (IRSA)" procedure has been introduced as a direct extension of the traditional RSA procedure (Aydınoğlu, 2003, 2004).

Despite the fact that pushover analysis has become extremely popular in recent years, there is still a lack of agreement on a universally accepted definition of the procedure. From a historical perspective, pushover analysis has always been understood as a nonlinear "capacity estimation tool" and generally called as "capacity analysis". The nonlinear structure is monotonically pushed by a set of forces with an invariant distribution until a predefined displacement limit at a given location (say, lateral displacement limit at the roof level of a building) is attained. Such predefined displacement limit is generally termed "target displacement". The structure may be further pushed up to the collapse condition in order to estimate its "ultimate" deformation and load carrying capacities. It is for this reason that pushover analysis has been also called as "collapse analysis".

However, in view of performance-based seismic assessment and design requirements, the above definition is not sufficient. According to the new concept introduced by Freeman et al. (1975) and Fajfar and Fischinger (1988), which was subsequently adopted in ATC 40 (ATC, 1996) and FEMA 273 (BSSC, 1997; FEMA, 2000), pushover analysis with its above-given historical definition represents only the first stage of a two-stage nonlinear static procedure, where it simply provides the nonlinear capacity curve of an equivalent single-degree-of-freedom (SDOF) system. The peak response, i.e., seismic demand, is then estimated through nonlinear analysis of this equivalent SDOF system under a given earthquake or through an inelastic displacement spectrum. In this sense the term "pushover analysis" now includes as well the estimation of the so-called "target displacement". Eventually, controlling seismic demand parameters, such as plastic hinge rotations, are obtained and compared with the specified limits (acceptance criteria) to verify the performance of the structure according to a given performance objective under a given earthquake. Thus according to this broader definition, pushover analysis is not only a capacity estimation tool, but at the same time it is a "demand estimation tool".

It is rather surprising that among the various multi-mode methods that appeared in the literature during the last decade, only two procedures, i.e., "Modal Pushover Analysis (MPA)" introduced by Chopra and Goel (2002) and "Incremental Response Spectrum Analysis (IRSA)" developed by Aydınoğlu (2003, 2004) conform to the above-given contemporary definition (for refined versions of MPA, see Hernandez-Montes et al. (2004), and Kalkan and Kunnath (2006)). Others have actually dealt with "structural capacity estimation" only, although this important limitation has been generally overlooked. It means that none of them aimed at estimating the nonlinear deformation demands (such as plastic hinge rotations or story drifts) under a given earthquake. Although elastic response spectrum of a specified earthquake was utilized, it was not for demand estimation, but only for scaling the relative contributions of vibration modes to obtain seismic load vectors (Antoniou et al., 2002; Elnashai, 2002; Gupta and Kunnath, 2000; Kalkan and Kunnath, 2004; Antoniou and Pinho, 2004a) or to obtain displacement vectors (Antoniou and Pinho, 2004b). Generally, building is pushed to a selected target displacement that is actually obtained from a nonlinear response history analysis (Gupta and Kunnath, 2000; Kalkan and Kunnath, 2004). Alternatively a pushover analysis is performed for a target building drift and the earthquake ground motion is scaled to match that drift (Antoniou and Pinho, 2004a, 2004b). Therefore the results are always presented in a relative manner, generally in the form of story displacement or story drift profiles where pushover and nonlinear response history analysis results are superimposed for a matching target displacement or building drift. Thus, such pushover procedures are able to estimate only the relative distribution of deformation demand quantities, not their magnitudes, and hence their role in a contemporary deformation-based seismic evaluation/design scheme is questionable.

In view of the above assessment, the main objective of this paper is to present the salient features of IRSA procedure (Aydınoğlu, 2003, 2004), which has been recently included in the Turkish Seismic Code (Ministry of Public Works and Settlement, 2006; Aydınoğlu, 2006) as a practical tool for performance-

based seismic assessment of existing buildings. But in a broader framework, the paper aims as well to provide a clear insight to the theoretical and practical aspects of the pushover analysis methods, in general. Towards this end, it will start with exploring the theoretical roots of the pushover methods, and will continue with the basic development and implementation of adaptive and invariant single-mode and multi-mode pushover procedures, including IRSA.

EXPLORING THE THEORETICAL ROOTS OF PUSHOVER ANALYSIS

As it is stated above, all pushover methods can be looked upon as nonlinear extensions of the Response Spectrum Analysis (RSA). In this direction, nonlinear response history analysis of a MDOF system will be treated in the following through a "piecewise linear process" where the nonlinear behavior is modeled by simple "plastic hinges".

1. Piecewise Linear Modeling of Nonlinear Response

Plastic hinges are zero-length elements through which the nonlinear behavior is assumed to be "concentrated" or "lumped" at predetermined sections. A typical plastic hinge is ideally located at the centre of a plastified zone called "plastic hinge length" to be defined at the each end of a clear length of a beam or column. A one-component plastic hinge model with or without strain hardening can be appropriately used to characterize a bi-linear moment-curvature relationship. The so-called "normality condition" can be used to account for the interaction between plastic axial and bending deformation components (McGuire et al., 2000).

Plastic hinge concept is ideally suited to the piecewise linear representation of concentrated nonlinear response. Linear behavior is assumed in between predetermined plastic hinge sections as well as temporally in between the formation of two consecutive plastic hinges. As part of a piecewise linearization process, yield surfaces of plastic hinge sections may be appropriately linearized, i.e., they may be represented by finite number of lines or planes in two- and three-dimensional response models, respectively. As an example, two-dimensional yield surfaces (lines) of reinforced concrete and wide flanged steel sections are shown in Figure 1. Note that number of linear segments may be increased in reinforced concrete section for an enhanced accuracy.

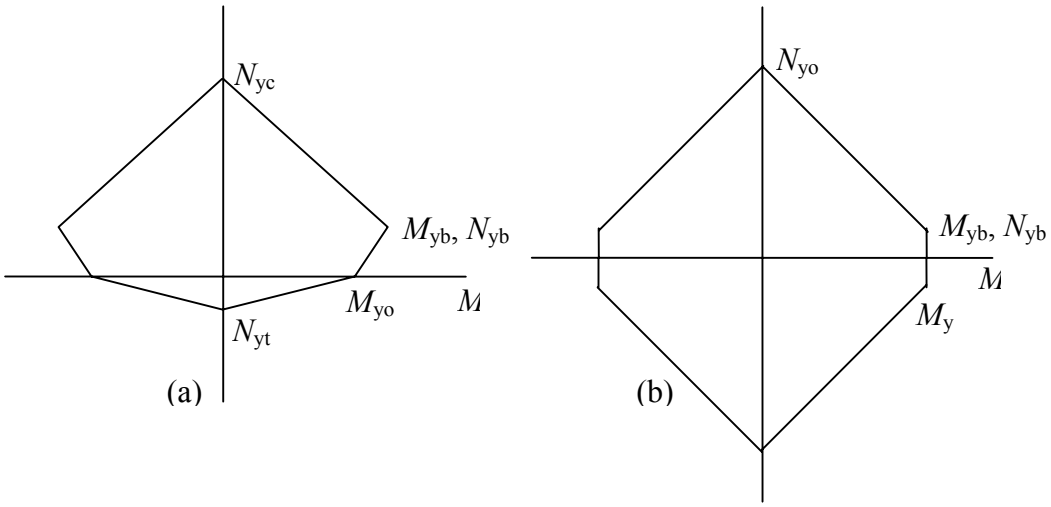

Fig. 1 Piecewise linearised yield surfaces (lines) of typical (a) reinforced concrete section, (b) wide flanged steel section

2. Piecewise Linear Equations of Motion of Nonlinear System

In a plastic hinge model with multi-linear hysteretic behavior, the dynamic response would be essentially linear during an incremental step (i) between a time t and a previous time station t_{i-1} at which the response is already determined. Thus, "piecewise linear" incremental equations of motion of a nonlinear multi-degree-of-freedom (MDOF) structure subjected to a uni-directional ground motion can be written for $t > t_{i-1}$ as

$$\mathbf{M}[\ddot{\mathbf{u}}(t)-\ddot{\mathbf{u}}(t_{i-1})]+\mathbf{C}^{(i)}[\dot{\mathbf{u}}(t)-\dot{\mathbf{u}}(t_{i-1})]+(\mathbf{K}^{(i)}-\mathbf{K}_{\mathrm{G}}^{(i)})[\mathbf{u}(t)-\mathbf{u}(t_{i-1})]=-\mathbf{M}\,\mathbf{I}_x^g[\ddot{u}_x^g(t)-\ddot{u}_x^g(t_{i-1})] \quad (1)$$

where $\mathbf{u}(t)$ represents the relative displacement vector and $\ddot{u}_x^g(t)$ refers to the ground acceleration of a given earthquake in *x*-direction. $\mathbf{I}_x^g$ is a kinematic vector representing the pseudo-static transmission of the ground acceleration to the structure, whose components associated with the degrees of freedom in *x* earthquake direction are unity and others are zero. In Equation (1), $\mathbf{M}$ denotes the mass matrix, $\mathbf{K}^{(i)}$ represents the instantaneous (tangent) stiffness matrix in incremental step (*i*) and $\mathbf{K}_G^{(i)}$ refers to geometric stiffness matrix accounting for second-order (P-delta) effects. The instantaneous damping matrix $\mathbf{C}^{(i)}$ is assumed to be Rayleigh type, i.e., it is formed as a linear combination of mass and stiffness matrices.

3. Piecewise Linear Mode-Superposition

The instantaneous displacement response during a piecewise linear incremental step (*i*) can be expanded to the modal coordinates as

$$\mathbf{u}(t)=\sum_{n=1}^{N_m}\mathbf{u}_n(t);\qquad \mathbf{u}_n(t)=\Phi_n^{(i)}\Gamma_{xn}^{(i)}\,d_n(t) \quad (2)$$

in which N_m refers to the number of modes to be considered in the modal expansion, $d_n(t)$ is the modal displacement, and $\mathbf{\Phi}_n^{(i)}$ is the instantaneous *n*th mode shape vector to be obtained from a free-vibration analysis:

$$(\mathbf{K}^{(i)}-\mathbf{K}_G^{(i)})\,\mathbf{\Phi}_n^{(i)}=(\omega_n^{(i)})^2\,\mathbf{M}\,\mathbf{\Phi}_n^{(i)} \quad (3)$$

where $\omega_n^{(i)}$ represents the instantaneous natural frequency. $\Gamma_{xn}^{(i)}$ in Equation (2) denotes the instantaneous participation factor for an earthquake in *x*-direction, which is defined as

$$\mathbf{\Gamma}_{xn}^{(i)}=\frac{L_{xn}^{(i)}}{M_n^{(i)}}=\frac{\mathbf{\Phi}_n^{(i)T}\mathbf{M}\,\mathbf{I}_x^g}{\mathbf{\Phi}_n^{(i)T}\mathbf{M}\,\mathbf{\Phi}_n^{(i)}} \quad (4)$$

Substituting Equation (2) and time derivatives into Equation (1) and pre-multiplying with $\mathbf{\Phi}_n^{(i)}$ followed by applying modal orthogonality conditions and considering Equation (4) result in an uncoupled instantaneous modal equation of motion in the *n*th mode:

$$\begin{aligned}\ddot{d}_n(t)+2\xi_n^{(i)}\omega_n^{(i)}\dot{d}_n(t)+(\omega_n^{(i)})^2 d_n(t)=&-[\ddot{u}_x^g(t)-\ddot{u}_x^g(t_{i-1})]\\&+\ddot{d}_n^*(t_{i-1})+2\xi_n^{(i)}\omega_n^{(i)}\dot{d}_n^*(t_{i-1})+(\omega_n^{(i)})^2 d_n^*(t_{i-1})\end{aligned} \quad (5)$$

Here, $\xi_n^{(i)}$ represents modal damping ratio, and $d_n^*(t_{i-1})$ is expressed as

$$d_n^*(t_{i-1})=\frac{\mathbf{\Phi}_n^{(i)T}\mathbf{M}\,\mathbf{u}(t_{i-1})}{L_{xn}^{(i)}} \quad (6)$$

where $L_{xn}^{(i)}$ is as defined in Equation (4). Equations (5) and (6) reveal that each modal equation is dependent upon the past response history of the MDOF structural system in terms of displacement vector and its time derivatives developed at the previous time instant. Applying modal expansion to $\mathbf{u}(t_{i-1})$ as in Equation (2), $d_n^*(t_{i-1})$ given in Equation (6) can be expressed as

$$d_n^*(t_{i-1})=\frac{\mathbf{\Phi}_n^{(i)T}\mathbf{M}\sum_{m=1}^{N_m}\mathbf{\Phi}_m^{(i-1)}\mathbf{\Gamma}_{xm}^{(i-1)}d_m(t_{i-1})}{L_{xn}^{(i)}} \quad (7)$$

from which it can be observed that if $\mathbf{\Phi}_n^{(i-1)}$ were close enough to $\mathbf{\Phi}_n^{(i)}$, the above-mentioned coupling would cease to exist. Indeed, if it is assumed that $\mathbf{\Phi}_n^{(i)}\cong\mathbf{\Phi}_n^{(i-1)}$ for all modes, which is expected to hold

in relatively "redundant" systems, then modal orthogonality conditions would result in the following simplification:

$$d_n^*(t_{i-1}) \cong d_n(t_{i-1}) \tag{8}$$

For the sake of simplicity, the following modified notation is used in all expressions to follow:

$$d_n(t_i) \rightarrow d_n^{(i)}; \qquad d_n(t_{i-1}) \rightarrow d_n^{(i-1)} \tag{9}$$

Thus from Equations (5), (8) and (9), typical *n*th modal equation can be expressed approximately in an incremental form as

$$\Delta\ddot{d}_n^{(i)} + 2\xi_n^{(i)}\omega_n^{(i)}\Delta\dot{d}_n^{(i)} + (\omega_n^{(i)})^2\Delta d_n^{(i)} = -\Delta\ddot{u}_x^{g(i)} \tag{10}$$

where $\Delta\ddot{u}_x^{g(i)} = \ddot{u}_x^{g(i)} - \ddot{u}_x^{g(i-1)}$ is the ground acceleration increment and $\Delta d_n^{(i)}$ represents the modal displacement increment, the latter of which can be expressed as

$$d_n^{(i)} = d_n^{(i-1)} + \Delta d_n^{(i)} \tag{11}$$

Note that the third term at the left-hand side of Equation (10) is called "modal pseudo-acceleration increment", which is defined as

$$\Delta a_n^{(i)} = (\omega_n^{(i)})^2\Delta d_n^{(i)} \tag{12}$$

where its cumulative value at the (*i*)th step can be written as similar to the cumulative modal displacement given in Equation (11):

$$a_n^{(i)} = a_n^{(i-1)} + \Delta a_n^{(i)} \tag{13}$$

Thus Equation (10) can be rewritten as

$$\Delta\ddot{d}_n^{(i)} + 2\xi_n^{(i)}\omega_n^{(i)}\Delta\dot{d}_n^{(i)} + \Delta a_n^{(i)} = -\Delta\ddot{u}_x^{g(i)} \tag{14}$$

With respect to the exact incremental equations of motion given in Equation (1), approximate modal incremental equations given in Equation (10) or (14) are expected to provide better results in relatively "redundant systems" due to the assumptions indicated in Equation (8). Such systems have the potential of developing large number of plastic hinges and therefore the formation of a new hinge would only marginally (or even negligibly) modify the mode shapes of the structural system. On the contrary, in structural systems where only a small number of hinges can potentially develop, such as bridges with few isolated single-column piers, the use of incremental equations of motion (see Equation (10) or (14)) could lead to erroneous results, because significant changes could occur in mode shapes in successive incremental steps. Note that these observations apply as well to those systems whose response is practically governed by a single mode only.

4. Modal Hysteresis Loops and Modal Capacity Diagrams

It is shown above that incremental solution of Equation (1) can be approximately reduced to the incremental solution of Equation (10) or (14), through which "modal displacement versus modal pseudo-acceleration diagrams" can be constructed. Those hypothetical diagrams represent the "modal hysteresis loops", which are schematically depicted in Figure 2(a). The outer hysteresis loops should be the fattest in the first mode and get thinner and steeper as the mode number increases. According to Equation (12), the instantaneous slope of a given diagram is equal to the eigenvalue (natural frequency squared) of the corresponding mode at the piecewise linear increment concerned. The backbone curves of the hypothetical modal hysteresis loops in the first quadrant may be appropriately called the "modal capacity diagrams", which are indicated by solid curves in Figure 2(a). In the special case where the first mode alone is assumed to represent the dynamic response, the modal capacity diagram is, by definition, identical to the so-called "capacity spectrum" defined in the Capacity Spectrum Method (ATC, 1996). The term "modal capacity diagram" is introduced by Aydınoğlu (2003) by adding the word "modal" to the terminology proposed by Chopra and Goel (1999). Note that in linearly elastic response, modal hysteresis curves and modal capacity diagrams degenerate into straight lines as shown in Figure 2(b).

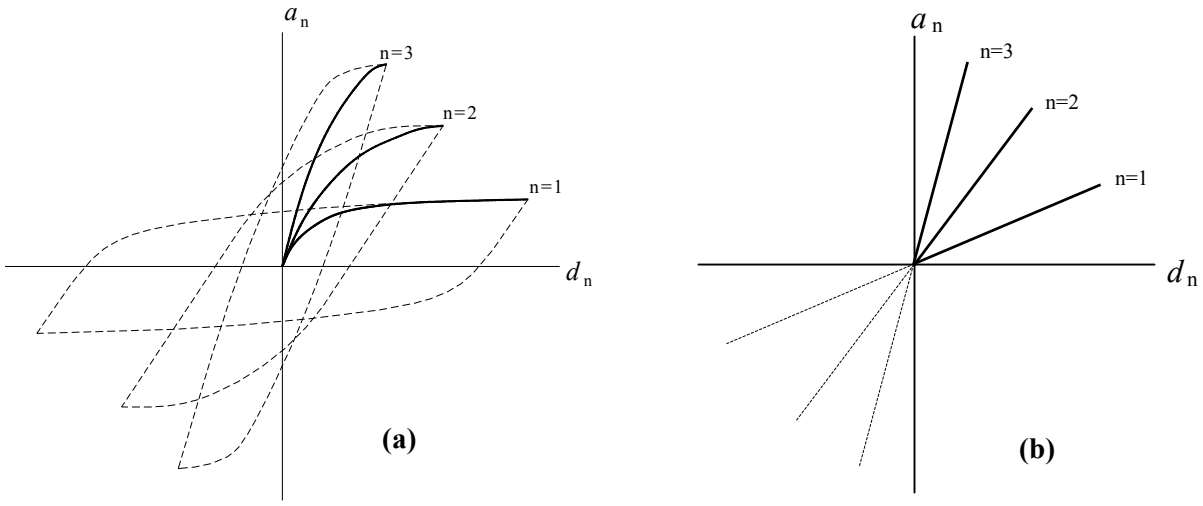

Fig. 2 (a) Schematic representation of hypothetical modal hysteresis loops and their backbone curves (modal capacity diagrams—solid curves); (b) Corresponding curves and diagrams in linear response

5. A Generic Definition of Pushover Analysis

Within the framework of the theoretical basis explained above, pushover analysis can be defined as a "monotonic nonlinear analysis" of progressively yielding MDOF system with a simultaneous "monotonic" construction of the modal capacity diagram(s) until the peak response is obtained for a given earthquake ground motion, so that the analysis procedure can be used as an essential tool in performance assessment process. Thus, according to the classification given in the introductory section of this paper, pushover analysis is ultimately defined as a "seismic demand estimation tool". More specifically, the analysis should be able to produce ductile deformation demands, such as plastic hinge rotations or corresponding strains, as well as brittle force demands, e.g., shears in reinforced concrete elements.

With respect to the above presented analytical formulation, now the analysis process is changed from a "dynamic response history analysis" of MDOF system to a "monotonic pushover history analysis", while the "incremental time step" (i) transforms to a monotonic "pushover step" (i), which is defined as the "analysis step in between the formation of two consecutive plastic hinges". Since modal capacity diagrams are defined as the backbone curves of the modal hysteresis loops, their peak values, i.e., modal seismic demand, can be obtained from the nonlinear solution of Equation (10) under a given earthquake ground motion. Alternatively, "inelastic response spectrum" can be utilized for the same purpose, which is the preferred option for routine engineering applications.

The "pushover history analysis" can be performed either in the form of a static analysis under the specified equivalent seismic loads with adaptive or invariant distributions, or it may be formulated as a piecewise linear response spectrum analysis by considering the continuously changing properties of the structure. The latter may be interpreted as performing pushover analyses in various modes simultaneously.

As a general background to pushover history analyses, relationships between the coordinates of modal capacity diagrams, i.e., modal displacement and modal pseudo-acceleration of modal SDOF systems versus the corresponding response quantities of the MDOF system, can be expressed as in the following:

(a) Piecewise linear relationship between the nth modal displacement increment and the corresponding displacement increment of MDOF system at the (i)th pushover step is

$$\Delta \mathbf{u}_n^{(i)} = \boldsymbol{\Phi}_n^{(i)} \boldsymbol{\Gamma}_{xn}^{(i)} \Delta d_n^{(i)} \tag{15}$$

(b) Piecewise linear relationship between the nth modal pseudo-acceleration increment and the corresponding equivalent seismic load increment of MDOF system at the (i)th pushover step is

$$\Delta \mathbf{f}_n^{(i)} = \mathbf{M}\,\boldsymbol{\Phi}_n^{(i)}\,\boldsymbol{\Gamma}_{xn}^{(i)}\,\Delta a_n^{(i)} \tag{16}$$

Note that the above expression is adopted from the monotonic counterpart of the third term on the left-hand side of Equation (1), which can be expressed as

$$\Delta \mathbf{f}_n^{(i)} = (\mathbf{K}^{(i)} - \mathbf{K}_G^{(i)})\,\Delta \mathbf{u}_n^{(i)} \tag{17}$$

In fact, substituting Equation (15) into Equation (17) and utilizing Equations (3) and (12) results in Equation (16).

SINGLE-MODE PUSHOVER ANALYSIS: PIECEWISE LINEAR IMPLEMENTATION WITH ADAPTIVE AND INVARIANT LOAD PATTERNS

Single-mode piecewise linear pushover procedure is applicable to low-to-medium rise regular buildings whose response is effectively controlled by the first (predominant) mode. Slight torsional irregularities may be allowed provided that a 3-D structural model is employed.

Regarding the adaptive pattern, the first-mode counterpart of equivalent seismic load increment given in Equation (16) can be written for the (*i*)th pushover step as

$$\Delta \mathbf{f}_1^{(i)} = \bar{\mathbf{m}}_1^{(i)}\,\Delta a_1^{(i)}; \qquad \bar{\mathbf{m}}_1^{(i)} = \mathbf{M}\,\boldsymbol{\Phi}_1^{(i)}\boldsymbol{\Gamma}_{x1}^{(i)} \tag{18}$$

where $\bar{\mathbf{m}}_1^{(i)}$ represents the vector of "participating modal masses" effective in the first mode. Superscript (*i*) on the participating modal mass and mode shape vectors as well as on the modal participation factor indicates that instantaneous first-mode shape corresponding to the current configuration of the structural system is considered following the formation of the last plastic hinge at the end of the previous pushover step. In adaptive case, a fully compatible modal expression can be written from Equation (15) for the increment of displacement vector as well:

$$\Delta \mathbf{u}_1^{(i)} = \bar{\mathbf{u}}_1^{(i)}\,\Delta d_1^{(i)}; \qquad \bar{\mathbf{u}}_1^{(i)} = \boldsymbol{\Phi}_1^{(i)}\boldsymbol{\Gamma}_{x1}^{(i)} \tag{19}$$

Since both $\Delta \mathbf{u}_1^{(i)}$ and $\Delta \mathbf{f}_1^{(i)}$ are based on the same instantaneous modal quantities, there is a one-to-one correspondence between them. Thus, adaptive implementation of the single-mode pushover analysis can be based on either a monotonic increase of displacements or equivalent seismic loads. However, this is not the case when the load pattern is kept invariant during pushover history, i.e., a compatible modal displacement expression cannot be provided. In the following paragraph, pushover analysis will be treated on the basis of monotonic increase in the equivalent seismic loads where both adaptive and invariant patterns will be considered in a common framework.

In the case of invariant load pattern, Equation (18) is modified as

$$\Delta \mathbf{f}_1^{(i)} = \bar{\mathbf{m}}_1^{(1)}\,\Delta a_1^{(i)}; \qquad \bar{\mathbf{m}}_1^{(1)} = \mathbf{M}\,\boldsymbol{\Phi}_1^{(1)}\boldsymbol{\Gamma}_{x1}^{(1)} \tag{20}$$

where the vector of first-mode participating modal masses, $\bar{\mathbf{m}}_1^{(1)}$, is defined at the first pushover step (i = 1) and retained "invariant" during the entire course of pushover history. Note that inverted triangular or even height-wise constant amplitude mode shapes are being used in practice (FEMA, 2000) in place of $\boldsymbol{\Phi}_1^{(1)}$.

1. Pushover History Analysis

In piecewise linear pushover history analysis equivalent seismic load vector of the MDOF system, which could have either adaptive or invariant pattern, is increased monotonically in the increments of $\Delta \mathbf{f}_1^{(i)}$ where modal pseudo-acceleration increment, $\Delta a_1^{(i)}$, is simultaneously calculated as the single unknown quantity at each (*i*)th pushover step leading to the formation of a new hinge. In this respect any response quantity of interest, such as the increment of an internal force, a displacement component, a story drift, or a plastic hinge rotation of a previously formed hinge, to be developed at the end of the (*i*)th pushover step may be written in a generic form as

$$q^{(i)} = q^{(i-1)} + \Delta q^{(i)} = q^{(i-1)} + \bar{q}^{(i)}\Delta a_1^{(i)} \tag{21}$$

Here, $q^{(i)}$ and $q^{(i-1)}$ are the "generic response quantities" to develop at the end of current and previous pushover steps, $\Delta q^{(i)}$ is the respective increment, and $\bar{q}^{(i)}$ represents a generic response quantity to be obtained for $\Delta a_1^{(i)} = 1$, i.e., from the application of $\bar{\mathbf{m}}_1^{(i)}$ or $\bar{\mathbf{m}}_1^{(1)}$ as equivalent seismic loads, representing the adaptive or invariant pattern, respectively. Now, the above generic expression is specialized for the response quantities that define the coordinates of the "yield surfaces" of all potential plastic hinges, e.g., biaxial bending moments and axial forces in a general, three-dimensional response of a framed structure. In the first pushover step (i = 1), response quantities due to gravity loading are considered as $q^{(0)}$ in Equation (21). As part of the piecewise linearization process of pushover analysis as well as to avoid iterative operations in the hinge identification process, yield surfaces are appropriately linearized in a piecewise fashion as mentioned above (Figure 1), i.e., they are represented by finite number of lines or planes in two- and three-dimensional response models, respectively. As an example, planar yield surfaces (lines) of a reinforced concrete or steel section (j) as shown in Figure 1 where a typical line (s) can be expressed as

$$\alpha_{j,s} M_{jp} + \beta_{j,s} N_{jp} = 1 \tag{22}$$

Here, M_{jp} and N_{jp} represent the yield bending moment and corresponding axial force, respectively, at the section j while $\alpha_{j,s}$ and $\beta_{j,s}$ refer to the coefficients defining the yield line (s). For the (i)th pushover step, Equation (21) is specialized for bending moment and axial force as

$$M_{j,1}^{(i)} = M_{j,1}^{(i-1)} + \bar{M}_{j,1}^{(i)} \Delta a_1^{(i)}; \qquad N_{j,1}^{(i)} = N_{j,1}^{(i-1)} + \bar{N}_{j,1}^{(i)} \Delta a_1^{(i)} \tag{23}$$

which are then substituted into Equation (22), and $\Delta a_1^{(i)}$ is extracted as

$$(\Delta a_1^{(i)})_{j,s} = \frac{1 - \alpha_{j,s} M_{j,1}^{(i-1)} - \beta_{j,s} N_{j,1}^{(i-1)}}{\alpha_{j,s} \bar{M}_{j,1}^{(i)} + \beta_{j,s} \bar{N}_{j,1}^{(i)}} \tag{24}$$

The yield line (s) at the section (j) that intersected with a minimum positive $(\Delta a_1^{(i)})_{j,s}$ among all yield lines of all potential plastic hinges identifies the new hinge formed at the end of the (i)th pushover step. Once $\Delta a_1^{(i)}$ is determined, any response quantity of interest developed at the end of that step can be obtained from the generic expression of Equation (21).

As the formation of the new hinge is identified, the current global stiffness matrix of the structure is locally modified such that only the element stiffness matrix affected by the new hinge is replaced with a new one for the next pushover step. Normality criterion is enforced in columns and walls for the coupling of internal forces as well as plastic deformation components of the newly formed plastic hinge.

Provided that the load pattern is adaptive and therefore resulting displacement increments are always compatible with the equivalent seismic load increments, modal displacement increment, $\Delta d_1^{(i)}$, is related through Equation (12) to the corresponding modal pseudo-acceleration increment, $\Delta a_1^{(i)}$, obtained at each pushover step:

$$\Delta d_1^{(i)} = \frac{\Delta a_1^{(i)}}{(\omega_1^{(i)})^2} \tag{25}$$

Here, $\omega_1^{(i)}$ represents the instantaneous natural circular frequency calculated at the (i)th pushover step. In the case of an invariant pattern, however, since modal equivalent loads and resulting displacement increments are not compatible, two procedures can be suggested to estimate the modal displacement increments.

(a) The first procedure involves the approximate calculation of the instantaneous eigenvalue, $(\omega_1^{(i)})^2$, as a Rayleigh quotient (Aydınoğlu, 2005):

$$(\omega_1^{(i)})^2 \cong \frac{\sum_k \bar{m}_{k,1}^{(1)}\ \bar{u}_{k,1}^{(i)}}{\sum_k m_k\ \bar{u}_{k,1}^{(i)\ 2}} \tag{26}$$

in which $\bar{u}_{k,1}^{(i)}$ represents the displacement component at the kth DOF under the equivalent seismic loads $\bar{m}_{k,1}^{(1)}$ with invariant pattern that are defined through Equation (20) for $\Delta a_1^{(i)} = 1$. Thus, the modal displacement increment, $\Delta d_1^{(i)}$, is obtained by substituting Equation (26) into Equation (25).

(b) The second procedure is the one already applied in practice (ATC, 1996; FEMA, 2000), where modal displacement increment is calculated through Equation (19), i.e., by specializing it for the roof displacement increment with the corresponding first-mode shape amplitude of the first pushover step:

$$\Delta d_1^{(i)} = \frac{\Delta u_{N,1}^{(i)}}{\Phi_{N,1}^{(1)}\ \Gamma_{x1}^{(1)}} \tag{27}$$

It is worth noting that in the single-mode pushover procedure presented herein, there is no need to plot the conventional pushover curve, with vertical axis representing the sum of equivalent seismic loads, i.e., base shear. Accordingly, conversion of the base shear increments to pseudo-acceleration increments is not required, because those are obtained directly by Equation (24) at each pushover step. In fact, it can be shown that even if the conventional approach had been applied the same results would be obtained, i.e., the base shear in x earthquake direction is obtained by summing up the equivalent seismic loads given by Equation (20) in that direction:

$$\mathbf{\Delta} V_{x1}^{(i)} = \mathbf{I}_x^{g\ T}\ \mathbf{\Delta f}_1^{(i)} = \mathbf{I}_x^{g\ T}\ \bar{\mathbf{m}}_1^{(1)}\ \mathbf{\Delta} a_1^{(i)} \tag{28}$$

On the other hand, total participating modal mass of the MDOF system in the x-direction is obtained by summing up the elements of the vector of participating masses given in Equation (20), i.e.,

$$\bar{M}_{x1}^{(1)} = \mathbf{I}_x^{g\ T}\ \bar{\mathbf{m}}_1^{(1)} = \frac{L_{x1}^{(1)\ 2}}{M_1^{(1)}} \tag{29}$$

Thus modal pseudo-acceleration increment at the (i)th pushover step is obtained from Equations (28) and (29) as

$$\mathbf{\Delta} a_1^{(i)} = \frac{\mathbf{\Delta} V_{x1}^{(i)}}{\bar{M}_{x1}^{(1)}} \tag{30}$$

which is nothing but the conversion relationship used in the traditional pushover procedure (ATC, 1996; FEMA, 2000).

With $\Delta d_1^{(i)}$ and $\Delta a_1^{(i)}$ determined as above, adding to those obtained at the end of the previous pushover step, modal displacement and modal pseudo-acceleration are calculated from Equations (11) and (13) at the end of the (i)th step as

$$d_1^{(i)} = d_1^{(i-1)} + \Delta d_1^{(i)}; \qquad a_1^{(i)} = a_1^{(i-1)} + \Delta a_1^{(i)} \tag{31}$$

It is noted that essentially $\Delta d_1^{(i)}$ and $\Delta a_1^{(i)}$ are the elements of an incremental modal equation of motion of the first-mode equivalent SDOF system:

$$\Delta \ddot{d}_1^{(i)} + 2\xi_1^{(i)}\omega_1^{(i)}\Delta \dot{d}_1^{(i)} + \Delta a_1^{(i)} = -\Delta i \ddot{u}_x^{g(i)} \tag{32}$$

Thus modal capacity diagram of the fundamental mode is obtained directly as shown schematically in Figure 3, which is nothing but the so-called "capacity spectrum" (ATC, 1996) obtained from the traditional pushover curve through a modal coordinate transformation. According to Equation (25), instantaneous slope of the linear segment of the modal capacity diagram at the pushover step (i) in between the plastic hinge points (i–1) and (i) is equal to the fundamental "eigenvalue" of the structural system at that step as shown in Figure 3.

Note that instantaneous slope of the capacity diagram could turn out to be negative due to the P-delta effects, as indicated in Figure 3, when accumulated plastic deformations result in a negative-definite

second-order stiffness matrix. In the case of invariant load pattern, at such a critical pushover step, the monotonic load increase process is terminated. From such a step onwards, analysis is generally continued with a monotonic displacement increment process, while retaining a constant displacement pattern obtained at the critical step. The accuracy of this approach is doubtful.

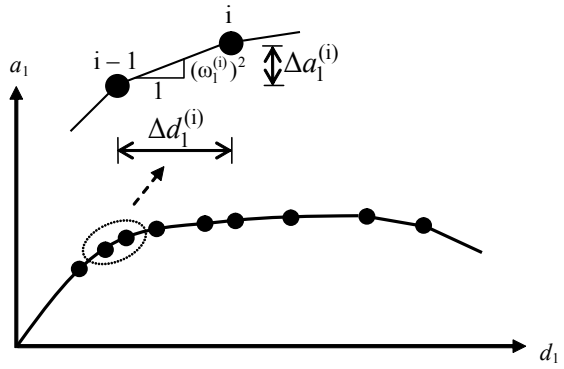

Fig. 3 Modal capacity diagram of the fundamental mode

In the case of adaptive solution, the analysis process is not influenced by a negative instantaneous slope of the capacity diagram. A negative slope means a negative eigenvalue and thus an imaginary natural frequency, which leads to a modal response that resembles the non-vibratory response of an over-damped system (Aydınoğlu and Fahjan, 2003). The corresponding mode shape has a remarkable physical significance, representing the post-buckling deformation state of the structure. Although structural engineers are not familiar with the negative (or zero) eigenvalues due to negative-definite (or singular) stiffness matrices, such eigenvalues and corresponding eigenvectors do exist, which can be routinely calculated by "matrix transformation methods" of eigenvalue analysis, such as the well-known "Jacobi Method" (Bathe, 1996).

As mentioned above, a remarkable aspect of the above-presented adaptive procedure is that it does not necessitate the plotting of conventional pushover curve in terms of base shear versus roof displacement. Instead, modal capacity diagram, which itself is the essential tool for the estimation of modal displacement demand, is obtained directly on including direct consideration of the P-delta effects.

2. Estimation of Modal Displacement Demand: Inelastic Spectral Displacement

The above-described process of pushover history analysis is continued until cumulative modal displacement calculated by Equation (31) exceeds the first-mode "inelastic spectral displacement". It means that the last pushover step has been reached, and, therefore, the modal displacement to develop at the end of this step, $d_1^{(p)}$ (superscript p stands for "peak"), is made equal to the inelastic spectral displacement, $S_{di,1}$:

$$d_1^{(p)} = S_{di,1} \tag{33}$$

This is followed by the calculation of the modal displacement increment in the last step (p):

$$\Delta d_1^{(p)} = S_{di,1} - d_1^{(p-1)} \tag{34}$$

The inelastic first-mode spectral displacement, $S_{di,1}$, can be calculated for a given ground motion record through nonlinear analysis of the modal SDOF system according to Equation (32) by considering hysteresis loops defined by the bi-linearized modal capacity diagram as the backbone curve (see Figure 4(b)). However for practical purposes, inelastic first-mode spectral displacement, $S_{di,1}$, can be appropriately defined through a simple procedure based on the "equal displacement rule" (FEMA, 2000):

$$S_{di,1} = C_{R,1} S_{de,1} \tag{35}$$

in which $S_{de,1}$ represents the elastic spectral displacement of the corresponding linear SDOF system with the same period (stiffness) as the initial period of the bilinear inelastic system. Note that in practice

cracked section stiffnesses are used in reinforced concrete systems throughout the pushover analysis and therefore the fundamental period of the system calculated at the first "linear" pushover step (i = 1) is taken as the initial period of the bilinear inelastic system. This is contrary to the traditional approach where the fundamental period is further lengthened excessively due to the bi-linearization of modal capacity diagram. In Figure 4, modal capacity diagram and the elastic response spectrum are combined in a "displacement—pseudo-acceleration" format. In the case where $T_1^{(1)} > T_S$ (with T_S being the characteristic spectrum period at the intersection of constant velocity and constant acceleration regions), bi-linearization of the modal capacity diagram is even unnecessary as indicated in Figure 4(a), because "spectral displacement amplification factor" $C_{R,1}$ is always equal to unity:

$$C_{R,1} = 1 \qquad (T_1^{(1)} > T_S) \tag{36}$$

In the case where $T_1^{(1)} \le T_S$, initial period is still defined as above; however, an iteration is necessary to calculate the spectral displacement amplification factor by using the following familiar relationship (FEMA, 2000; MPWS, 2006):

$$C_{R,1} = \frac{1 + (R_{y,1} - 1)T_S / T_1^{(1)}}{R_{y,1}} \ge 1 \qquad (T_1^{(1)} \le T_S) \tag{37}$$

in which $R_{y,1}$ refers to the yield reduction factor (Figure 4(b)):

$$R_{y,1} = \frac{S_{ae,1}}{a_{y,1}} \tag{38}$$

Note that alternative relationships are available for the displacement amplification factor that can be used in practical applications in lieu of those given by Equations (36) and (37). For those reference may be given to Aydınoğlu and Kaçmaz (2002), and to FEMA 440 (FEMA, 2005).

Once modal displacement increment in the last step, $\Delta d_1^{(p)}$, is estimated, the corresponding $\Delta a_1^{(p)}$ is determined, and in turn, any response quantity of interest developed at the end of that step can be obtained from the generic expression of Equation (21).

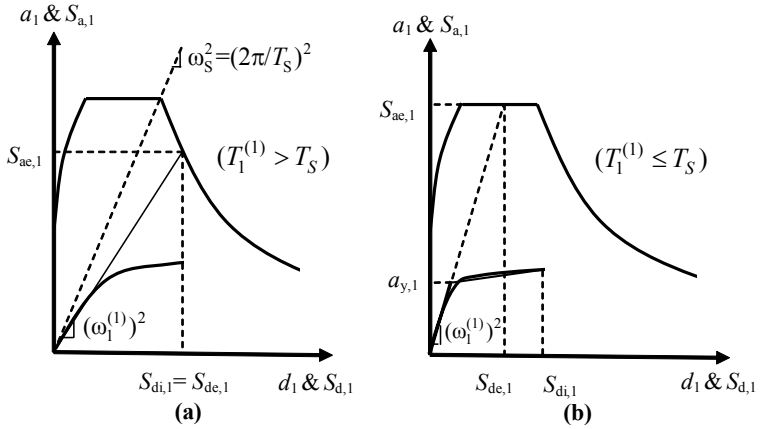

Fig. 4 Estimating modal displacement demand

MULTI-MODE ADAPTIVE PUSHOVER ANALYSIS: INCREMENTAL RESPONSE SPECTRUM ANALYSIS (IRSA) PROCEDURE

Multi-mode pushover procedure is intended for application on high-rise and/or irregular buildings and bridges where the seismic response cannot be effectively represented by the first mode only. These include torsionally sensitive buildings with 3-D response characteristics.

In line with the theoretical background provided above, in the multi-mode case monotonic pushover history analyses have to be performed "simultaneously" in all the modes considered. As with the single-mode pushover, in the adaptive case both MDOF system displacement increments and equivalent seismic load increments are based on the same instantaneous modal quantities. Thus the implementation of multi-mode pushover analysis can be based on either a monotonic increase of displacements or equivalent seismic loads. These may be called "displacement-controlled" and "force-controlled" pushovers, respectively. To start with, using Equation (15), modal displacement increments of MDOF system can be expressed as

$$\Delta \mathbf{u}_n^{(i)} = \bar{\mathbf{u}}_n^{(i)} \Delta d_n^{(i)} \; ; \qquad \bar{\mathbf{u}}_n^{(i)} = \boldsymbol{\Phi}_n^{(i)} \boldsymbol{\Gamma}_{xn}^{(i)} \tag{39}$$

and corresponding expressions for the compatible seismic load increments can be written as multi-mode counterparts of those given in Equation (18) as

$$\Delta \mathbf{f}_n^{(i)} = \bar{\mathbf{m}}_n^{(i)} \Delta a_n^{(i)}; \qquad \bar{\mathbf{m}}_n^{(i)} = \mathbf{M} \boldsymbol{\Phi}_n^{(i)} \boldsymbol{\Gamma}_{xn}^{(i)} \tag{40}$$

1. Modal Scaling

In order to define modal MDOF response, modal displacement increments $\Delta d_n^{(i)}$ or modal pseudo-acceleration increments $\Delta a_n^{(i)}$ have to be determined in all modes at each pushover step, depending on whether displacement- or force-controlled pushover is applied. Since just a single plastic hinge forms and therefore only one yield condition is applicable at the end of each piecewise linear step, a reasonable assumption needs to be made for the relative values of modal displacement or modal pseudo-acceleration increments, so that the number of unknowns are reduced to one. This is called "modal scaling", which is the most critical assumption to be made in all multi-mode pushover procedures, including IRSA. In this respect the only exception is the Modal Pushover Analysis—MPA (Chopra and Goel, 2002) where modal coupling is completely disregarded in the formation of plastic hinges and therefore modal scaling is omitted.

1.1 Modal Scaling Based on Instantaneous Elastic Spectral Quantities

Modal scaling is probably the most critical and, at the same time, one of the most controversial issues of multi-mode pushover analysis. In a number of studies, such as Gupta and Kunnath (2000), Elnashai (2002), Antoniou et al. (2002), Antoniou and Pinho (2004a), force-controlled pushover is implemented where modal scaling is performed on "instantaneous" modal pseudo-accelerations. Using the terminology and notation of the present paper such a modal scaling can be expressed as

$$\Delta a_n^{(i)} = \Delta F^{(i)} S_{aen}^{(i)} \tag{41}$$

where $S_{aen}^{(i)}$ represents the instantaneous *n*th mode "elastic" spectral pseudo-acceleration at the (*i*)th pushover step, and $\Delta F^{(i)}$ refers to an incremental scale factor, which is independent of the mode number. Thus Equation (41) means that modal pseudo-acceleration increments are scaled in proportion to the respective elastic spectral accelerations. Note that the above-defined modal scaling is essentially identical to the scaling of modal displacement increments in proportion to respective elastic spectral displacements, which may be expressed as

$$\Delta d_n^{(i)} = \Delta F^{(i)} \; S_{den}^{(i)} \tag{42}$$

where $S_{den}^{(i)}$ represents the instantaneous *n*th mode "elastic" spectral displacement corresponding to the above-given $S_{aen}^{(i)}$, i.e., $S_{aen}^{(i)} = (\omega_n^{(i)})^2 S_{den}^{(i)}$. Such a scaling has been used recently in a displacement-controlled pushover procedure (Antoniou and Pinho, 2004b).

Naturally this type of modal scaling is exact for a single-step linear analysis with $\Delta F^{(1)} = 1$; however it is doubtful whether it should be implemented in a nonlinear case. In fact, instantaneous elastic spectral parameters have no relation at all with the instantaneous nonlinear modal response increments. When the structure softens due to accumulated plastic deformations, the instantaneous "elastic" spectral displacement of the first mode increases disproportionately with respect to those of the higher modes,

leading to an exaggeration of the effect of the first mode in the hinge formation process prior to reaching the peak response.

1.2 Modal Scaling Based on Instantaneous Inelastic Spectral Displacements

Displacement-controlled pushover is the preferred approach in the Incremental Response Spectrum Analysis—IRSA (Aydınoğlu, 2003, 2004), and modal pushovers are implemented simultaneously by imposing instantaneous displacement increments of the MDOF system at each pushover step according to Equation (39). In principle, modal displacements are scaled in IRSA with respect to the "inelastic spectral displacements", $S_{din}^{(i)}$, associated with the "instantaneous" configuration of the structure (Aydınoğlu, 2003). This is the main difference between IRSA and other studies referred to above where modal scaling is based on "instantaneous elastic" spectral pseudo-accelerations or displacements. IRSA's adoption of "inelastic spectral displacements" for modal scaling may be considered as a "rational choice", because those spectral displacements are nothing but the "peak" values of the modal displacements to be reached, as will be shown in the following.

In practice, modal scaling based on "inelastic spectral displacements" can be easily achieved by taking advantage of the "equal displacement rule". Assuming that seismic input is defined via "smoothed elastic response spectrum", according to this simple and well-known rule (which is already utilized above for the estimation of modal displacement demand in single-mode pushover), "peak displacement" of an inelastic SDOF system and that of the corresponding elastic system are assumed practically equal to each other, provided that the effective initial period is longer than the "characteristic period" of the elastic response spectrum. The characteristic period is approximately defined as the transition period from the constant acceleration segment to the constant velocity segment of the spectrum. For periods shorter than the characteristic period, elastic spectral displacement is amplified using a displacement modification factor, i.e., C_1 coefficient given in FEMA 356 (FEMA, 2000). However, such a situation is seldom encountered in mid- to high-rise buildings and long bridges involving multi-mode response. In such structures, effective initial periods of the first few modes are likely to be longer than the characteristic period and therefore those modes automatically qualify for the equal displacement rule. On the other hand, effective post-yield slopes of the modal capacity diagrams get steeper and steeper in higher modes with gradually diminishing inelastic behavior (Figure 5). Thus, it can be comfortably assumed that inelastic spectral displacement response in higher modes would not be different from the corresponding spectral elastic response. Hence, smoothed elastic response spectrum may be used in its entirety for scaling modal displacements without any modification. As in the single-mode analysis, in reinforced concrete buildings elastic periods calculated at the first pushover step may be considered in lieu of the initial periods obtained from the bi-linearization of modal capacity diagrams (see Figure 4(b)).

In line with the "equal displacement rule", scaling procedure applicable to the *n*th mode increment of modal displacement at the (*i*)th pushover step is simply expressed as

$$\Delta d_n^{(i)} = \Delta \tilde{F}^{(i)} S_{den}^{(1)} \tag{43}$$

where $\Delta \tilde{F}^{(i)}$ is an "incremental scale factor", which is applicable to all modes at the (*i*)th pushover step. $S_{den}^{(1)}$ represents the "initial elastic spectral displacement" defined at the first step (Figure 5), which is taken equal to the "inelastic spectral displacement" associated with the "instantaneous" configuration of the structure at any pushover step. Cumulative modal displacement at the end of the same pushover step can then be written as

$$d_n^{(i)} = \tilde{F}^{(i)} S_{den}^{(1)} \tag{44}$$

in which $\tilde{F}^{(i)}$ represents the "cumulative scale factor" with a maximum value of unity:

$$\tilde{F}^{(i)} = \tilde{F}^{(i-1)} + \Delta \tilde{F}^{(i)} \le 1 \tag{45}$$

Note that the modal scaling expressions given above correspond to a monotonic increase of the elastic response spectrum progressively at each step with a cumulative scale factor increasing from zero until unity. Physically speaking, the structure is being pushed such that at every pushover step modal displacements of all modes are increased by increasing elastic spectral displacements, defined at the first step ($i = 1$) in the same proportion (according to the "equal displacement rule"), until they simultaneously reach the target "spectral displacements" on the response spectrum. Shown in Figure 5 are the scaled

spectra corresponding to the first yield, to an intermediate pushover step ($\tilde{F}^{(i)} < 1$), and to the final step ($\tilde{F}^{(i)} = 1$), which are plotted in the ADRS (Acceleration-Displacement Response Spectrum) format and superimposed onto the modal capacity diagrams.

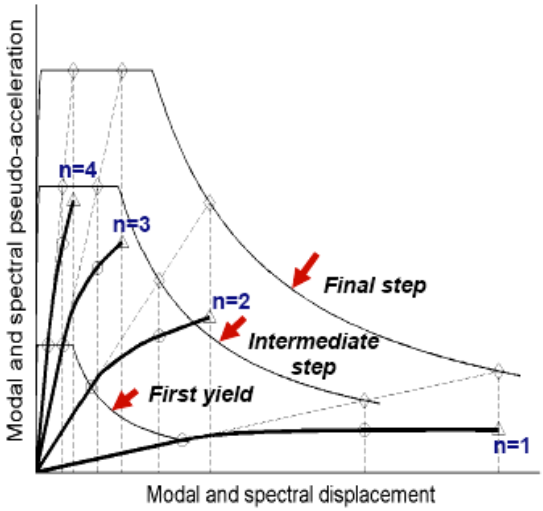

Fig. 5 Scaling of modal displacements through monotonic scaling of response spectrum

It is worth warning that the equal displacement rule may not be valid at near-fault situations with forward directivity effect.

Again, it needs to be stressed that IRSA is a "displacement-controlled" procedure and, therefore, the above-mentioned monotonic spectrum scaling applies to spectral displacements only, not to the elastic spectral pseudo-accelerations. For the sake of completeness, however, a "compatible" modal pseudo-acceleration increment, $\Delta a_n^{(i)}$, corresponding to the increment of "scaled" modal displacement may be defined from Equations (12) and (43) as

$$\Delta a_n^{(i)} = \Delta \tilde{F}^{(i)} S_{ain}^{(i)}; \qquad S_{ain}^{(i)} = \frac{(\omega_n^{(i)})^2}{(\omega_n^{(1)})^2} S_{aen}^{(1)} \tag{46}$$

where $S_{ain}^{(i)}$ represents "compatible inelastic spectral pseudo-acceleration", and $S_{aen}^{(1)}$ refers to "initial elastic spectral pseudo-acceleration" corresponding to the elastic spectral displacement, $S_{den}^{(1)}$, defined at the first pushover step.

2. Multi-mode Pushover History Analysis: Simultaneous Pushovers in All Modes and Modal Combination

Substituting Equation (43) into Equation (15) leads to the following expression for the displacement vector increment in the *n*th mode at the (*i*)th pushover step:

$$\Delta \mathbf{u}_n^{(i)} = \tilde{\mathbf{u}}_n^{(i)} \Delta \tilde{F}^{(i)}; \qquad \tilde{\mathbf{u}}_n^{(i)} = \Phi_n^{(i)} \Gamma_{xn}^{(i)} S_{den}^{(1)} \tag{47}$$

Utilizing Equations (16) and (46), equivalent seismic load vector increment corresponding to the displacement vector increment given above in Equation (47) may be written for an alternative load-controlled process:

$$\Delta \mathbf{f}_n^{(i)} = \tilde{\mathbf{f}}_n^{(i)} \Delta \tilde{F}^{(i)}; \qquad \tilde{\mathbf{f}}_n^{(i)} = \mathbf{M} \Phi_n^{(i)} \Gamma_{xn}^{(i)} S_{ain}^{(i)} \tag{48}$$

in which $S_{ain}^{(i)}$ is the compatible inelastic spectral pseudo-acceleration defined by Equation (46).

Now, piecewise linear multi-mode pushover history analysis can be performed at a given pushover step (*i*), by monotonically imposing displacement increments $\Delta \mathbf{u}_n^{(i)}$ of the MDOF system, as defined in Equation (47), or alternatively, by applying equivalent seismic load increments $\Delta \mathbf{f}_n^{(i)}$ given by

Equation (48) "simultaneously in all modes" considered. In this process, the increment of a "generic response quantity" of interest, such as the increment of an internal force, a displacement component, a story drift or the plastic rotation of a previously developed plastic hinge, may be calculated in each mode as

$$\Delta r_n^{(i)} = \tilde{r}_n^{(i)} \Delta \tilde{F}^{(i)} \tag{49}$$

where $\tilde{r}_n^{(i)}$ represents the generic response quantity to be obtained in each mode for $\Delta \tilde{F}^{(i)} = 1$, i.e., by imposing the displacement vector $\tilde{\mathbf{u}}_n^{(i)}$ given in Equation (47), or alternatively, by applying the load vector $\tilde{\mathbf{f}}_n^{(i)}$ given in Equation (48). Incremental scale factor $\Delta \tilde{F}^{(i)}$ is the single unknown at each pushover step leading to the formation of a new plastic hinge.

In the next stage, modal generic response quantity increments are combined by an appropriate modal combination rule, such as the Complete Quadratic Combination (CQC) rule as

$$\tilde{r}^{(i)} = \sqrt{\sum_{m=1}^{N_m} \sum_{n=1}^{N_m} (\tilde{r}_m^{(i)} \rho_{mn}^{(i)} \tilde{r}_n^{(i)})} \tag{50}$$

where $\rho_{mn}^{(i)}$ is the cross-correlation coefficient of the CQC rule. Thus, generic response quantity at the end of the (i)th pushover step can be estimated as

$$r^{(i)} = r^{(i-1)} + \Delta r^{(i)} = r^{(i-1)} + \tilde{r}^{(i)} \Delta \tilde{F}^{(i)} \tag{51}$$

in which $r^{(i)}$ and $r^{(i-1)}$ are the "generic response quantities" to develop at the end of current and previous pushover steps, respectively. In the first pushover step (i = 1), response quantities due to gravity loading are considered as $r^{(0)}$.

The next stage of multi-mode pushover history analysis is similar to the single-mode analysis where the above-given generic expression is specialized for the response quantities that define the coordinates of the "yield surfaces" of all potential plastic hinges, e.g., biaxial bending moments and axial forces in a general, three-dimensional response of a framed structure. As part of the piecewise linearization process of pushover analysis as well as to avoid iterative operations in the hinge identification process, yield surfaces are appropriately linearized in a piecewise fashion as mentioned above (Figure 1), i.e., they are represented by finite number of lines or planes in two- and three-dimensional response models, respectively. As an example, planar yield surfaces (lines) of a reinforced concrete or steel section (j) are shown in Figure 1 where a typical line (s) can be expressed as

$$\alpha_{j,s} M_{jp} + \beta_{j,s} N_{jp} = 1 \tag{52}$$

in which M_{jp} and N_{jp} represent the yield bending moment and corresponding axial force, respectively, at section j while $\alpha_{j,s}$ and $\beta_{j,s}$ refer to the coefficients defining the yield line (s). For the (i)th pushover step, Equation (51) is specialized for bending moment and axial force as

$$M_{j,1}^{(i)} = M_{j,1}^{(i-1)} + \tilde{M}_{j,1}^{(i)} \Delta \tilde{F}^{(i)}; \qquad N_{j,1}^{(i)} = N_{j,1}^{(i-1)} + \tilde{N}_{j,1}^{(i)} \Delta \tilde{F}^{(i)} \tag{53}$$

which are then substituted into Equation (52) and $\Delta \tilde{F}^{(i)}$ is extracted as

$$(\Delta \tilde{F}^{(i)})_{j,s} = \frac{1 - \alpha_{j,s} M_{j,1}^{(i-1)} - \beta_{j,s} N_{j,1}^{(i-1)}}{\alpha_{j,s} \tilde{M}_{j,1}^{(i)} + \beta_{j,s} \tilde{N}_{j,1}^{(i)}} \tag{54}$$

The yield line (s) at section (j) that intersected with a minimum positive $(\Delta \tilde{F}^{(i)})_{j,s}$ among all yield lines of all potential plastic hinges identifies the new hinge formed at the end of the (i)th pushover step.

Once $\Delta \tilde{F}^{(i)}$ is determined, any response quantity of interest developed at the end of that step can be obtained from the generic expression of Equation (51). Modal displacement increment $\Delta d_n^{(i)}$ in any mode can be obtained from Equation (43), and in turn, modal pseudo-acceleration increment from Equation (12), leading to the simultaneous estimation of respective cumulative quantities, i.e., the new coordinates of all modes, which can be obtained through Equations (11) and (13).

As mentioned in the case of single-mode pushover, when the formation of the new hinge is identified, the current global stiffness matrix of the structure is locally modified such that only the element stiffness matrix affected by the new hinge is replaced with a new one for the next pushover step. The normality criterion is enforced in columns and walls for the coupling of internal forces as well as plastic deformation components of the newly formed plastic hinge.

Thus it is seen that multi-mode pushover history analysis with IRSA is the extension of single-mode pushover history analysis described earlier. Indeed, instead of running a static analysis under equivalent seismic loads at each step, a response spectrum analysis is performed in IRSA at each step where seismic input data is specified either in the form of initial spectral displacement in each mode, $S_{den}^{(1)}$ (which is calculated in the first pushover step and remains unchanged at all pushover steps), or seismic input is given in terms of "compatible inelastic spectral pseudo-acceleration" $S_{ain}^{(i)}$ defined by Equation (46).

3. Estimation of Peak Quantities: Inelastic Seismic Demand

The above-described "pushover-history" process is repeated for all pushover steps until cumulative spectrum scale factor defined by Equation (45) exceeds unity at the end of a given pushover step. When such a step is detected, which is indicated by superscript (p), incremental scale factor corresponding to this final pushover step is re-calculated from Equation (45) as

$$\Delta\tilde{F}^{(p)} = 1 - \tilde{F}^{(p-1)} \tag{55}$$

In the last pushover step, modal displacement increment is redefined as

$$\Delta d_n^{(p)} = C_{Rn} S_{den}^{(1)} \Delta\tilde{F}^{(p)} \tag{56}$$

where C_{Rn} represents "spectral displacement amplification factor" in the nth mode. If $C_{Rn} > 1$, then seismic input for the nth mode is modified from $S_{den}^{(1)}$ to $C_{Rn} S_{den}^{(1)}$, and the generic response quantity $\tilde{r}_j^{(p)}$ is recalculated at the last step by repeating the elastic response spectrum analysis. Finally peak value of any response quantity of interest is obtained from the generic expression of Equation (51) for $i = p$:

$$r^{(p)} = r^{(p-1)} + \Delta r^{(p)} = r^{(p-1)} + \tilde{r}^{(p)} \Delta\tilde{F}^{(p)} \tag{57}$$

Spectral displacement amplification factor C_{Rn} is calculated as shown below.

If $T_n^{(1)} > T_B$, i.e., $(\omega_n^{(1)})^2 < \omega_B^2$, then C_{Rn} = 1. If $T_n^{(1)} < T_B$, i.e., $(\omega_n^{(1)})^2 > \omega_B^2$, then C_{Rn} is determined approximately as (MPWS, 2006)

$$\begin{aligned} C_{Rn} &= \frac{1 + (R_{yn} - 1) T_B / T_n^{(1)}}{R_{yn}} \geq 1 \qquad (\lambda_n^{(p)} \leq 0.10) \\ C_{Rn} &= \frac{1 + (R_{yn} - 1) T_B / T_n^{(1)}}{10 \lambda_n^{(p)} R_{yn}} \geq 1 \qquad (\lambda_n^{(p)} > 0.10) \end{aligned} \tag{58}$$

where R_{yn} is the nth mode yield reduction factor as defined below, i.e., the nth mode counterpart of the first mode yield reduction factor defined in Equation (38) (Figure 4(b)). Post-yield slope $\lambda_n^{(p)}$ is also defined below:

$$R_{yn} = \frac{S_{aen}^{(1)}}{a_{yn}}; \; \lambda_n^{(p)} = \frac{(\omega_n^{(p)})^2}{(\omega_n^{(1)})^2} \tag{59}$$

Note that the second spectral displacement amplification factor given in Equation (58) is intended for higher modes with shorter natural periods where inelastic spectral displacements would be reduced due to steeper post-yield slopes of higher-mode capacity diagrams (Önem, 2006).

4. Treatment of P-Delta Effects in IRSA

P-delta effects are rigorously considered in IRSA through straightforward consideration of geometric stiffness matrix in each increment of the response spectrum analysis performed. Along the pushover-

history process, accumulated plastic deformations result in negative-definite second-order stiffness matrices, which in turn yield negative eigenvalues, and hence, negative post-yield slopes in the modal capacity diagrams of the lower modes. The corresponding mode shapes are representative of the post-buckling deformation state of the structure, which may significantly affect the distribution of internal forces and inelastic deformations of the structure.

Analysis of inelastic SDOF systems based on bilinear backbone curves with negative post-yield slopes indicate that such systems are susceptible to "dynamic instability" rather than having amplified displacements due to the P-delta effects. Therefore, the use of P-delta amplification coefficient (C_3) defined in FEMA 356 (FEMA, 2000) is no longer recommended (FEMA, 2005). The dynamic instability is known to depend on the yield strength, initial stiffness, negative post-yield stiffness, and the hysteretic model of SDOF oscillator as well as on the characteristics of the earthquake ground motion. Accordingly, practical guidelines have been proposed for the minimum strength limits in terms of other parameters to avoid instability (Miranda and Akkar, 2003; FEMA, 2005). Further research is needed for the realistic cases of backbone curves resulting from modal capacity diagrams, which exhibit multiple post-yield slopes with both ascending and descending branches. For the time being, equal displacement rule is used in IRSA, even when P-delta effects are present, as long as an imminent danger of dynamic instability is not expected according to the above-mentioned practical guidelines.

5. Summary of IRSA

The analysis stages to be applied at each piecewise linear pushover step (i) of IRSA are summarized below:

(1) Run a linear response spectrum analysis (RSA) with a sufficient number of modes by considering instantaneous second-order stiffness matrix corresponding to the current plastic hinge configuration. RSA at each step actually corresponds to performing simultaneous pushover analyses in all modes for a unit value of incremental scale factor $\Delta\tilde{F}^{(i)}$. In running RSA, the seismic input is specified in terms of initial spectral displacements $S_{den}^{(1)}$, which would be the same at all pushover steps according to the "equal displacement rule". They are calculated only once at the first pushover step as elastic spectral displacements. Alternatively, compatible spectral pseudo-accelerations $S_{ain}^{(i)}$ defined at each step by Equation (46) may be specified as seismic input. All response quantities of interest, $r^{(i)}$, are obtained by applying an appropriate modal combination rule (e.g., CQC rule in Equation (50)).

(2) Specialize the generic expression of Equation (51) for the response quantities that define the coordinates of the yield surfaces of all potential plastic hinges, i.e., biaxial bending moments and axial forces in a general, three-dimensional response of a framed structure. Response quantities due to the gravity loading are considered as $r^{(0)}$ at the first pushover step. Calculate the incremental scale factor $\Delta\tilde{F}^{(i)}$ according to the yield conditions of all potential plastic hinges and identify the new yielded hinge.

(3) Calculate cumulative scale factor $\tilde{F}^{(i)}$ from Equation (45) and check if it exceeded unity. If exceeded, calculate the incremental scale factor $\Delta\tilde{F}^{(p)}$ from Equation (55) for the final pushover step and carry on according to Equations (56)–(59). If not, continue with the next stage.

(4) Calculate all response quantities of interest developed at the end of the pushover step from the generic expression of Equation (51). If the final pushover step has been reached, terminate the analysis. If not, continue with the next stage.

(5) Modify the current second-order stiffness matrix by considering the last yielded hinge identified at Stage (2) and return to Stage (1) for the next pushover step.

6. Special Cases

Single-mode adaptive pushover analysis presented earlier in this paper is a special case of IRSA with n = 1. Since no modal scaling is involved in the single-mode analysis, the incremental scale factor $\Delta\tilde{F}^{(i)}$ becomes directly proportional to the modal displacement increment $\Delta d_1^{(i)}$ as follows (see Equation (43)):

$$\Delta\tilde{F}^{(i)} = \frac{\Delta d_1^{(i)}}{S_{de1}^{(1)}} \tag{60}$$

On the other hand, when large values are assigned for yield moments such that no plastic hinging occurs, IRSA automatically degenerates to the linear response spectrum analysis (RSA) (see Figure 2(b)). These two special cases confirm the generality of the IRSA procedure.

FURTHER OBSERVATIONS ON OTHER PUSHOVER PROCEDURES

For the sake of completeness in covering the multi-mode pushover procedures, two classes of methods are briefly highlighted.

1. Multi-mode Pushover Analysis with Combined Seismic Loads or Displacements

It is interesting to note that in a number of multi-mode pushover procedures, e.g., Elnashai (2002), Antoniou et al. (2002), Antoniou and Pinho (2004a, 2004b), which employ modal scaling based on "instantaneous" elastic spectral quantities (see the discussion on "modal scaling" above), scaled seismic loads or displacements are combined with a modal combination rule, normalized, and then are applied to the structure at each step to obtain the increments of "combined" pushover curve coordinates. Note that a pitfall is inherent in these procedures regarding the application of the modal combination in defining applied loads or displacements instead of combining the individual response quantities induced by those loads or displacements in each mode (see Chopra, 2001). Thus, individual modal capacity diagrams cannot be defined, and consequently, modal peaks and hence seismic demand quantities cannot be obtained for a given earthquake, as discussed earlier.

2. Multi-mode Pushover Analysis without Modal Scaling: Modal Pushover Analysis (MPA)

It is worth noting that one of the methods for multi-mode pushover analysis, namely Modal Pushover Analysis (MPA), which was developed by Chopra and Goel (2002) based upon earlier studies (Paret et al., 1996; Sasaki et al., 1998), completely ignores the modal contributions to the section forces in the formation of plastic hinges. Nonlinear response is estimated independently for each mode with a single-mode pushover analysis based on an invariant load pattern proportional to the initial linear elastic mode shape of a given mode. Since modal coupling is ignored, modal scaling is not required. Peak response quantities, i.e., modal demands, are obtained for each mode from a SDOF system analysis independently, and are then combined (exactly as in the linear response spectrum analysis) with an appropriate modal combination rule. It is reported that the above-described MPA procedure is able to estimate story drifts with a reasonable accuracy (Chopra and Goel, 2002). However it fails to estimate the locations of plastic hinges as well as the plastic hinge rotations and section forces, the essential demand quantities for performance assessment in ductile and brittle behaviour modes, for which supplementary analyses are needed (Goel and Chopra, 2004, 2005). Recently certain refinements have been made on MPA through energy-based development of modal capacity diagrams (Hernandez-Montes et al., 2004; Kalkan and Kunnath, 2006).

EXAMPLES

Several examples have already been presented on IRSA applications in previously published material (see Aydınoğlu, 2003, 2004). In this paper, some of the results of an ongoing parametric study (Önem and Aydınoğlu, 2006) are presented. The 8-, 12-, 16- and 20-storey reinforced concrete frames shown in Figure 6 were designed to Turkish Seismic Code (MPWS, 2006) provisions with the characteristics given in Table 1. For nonlinear response history analysis, 20 real records with earthquake magnitude between 6.0 and 7.5 were employed (Table 2). The records were appropriately scaled to match a smoothed elastic response spectrum that was also used in the multi-mode pushover analysis by IRSA (Figure 7). Results of the nonlinear response history analysis (NRHA), 4-mode IRSA, and single-mode IRSA are presented in terms of mean values of story displacements, inter-story drift ratios, and plastic hinge rotations of central span beams, as shown in Figures 8, 9, and 10, respectively. The differences between the multi-mode and single-mode pushover analyses are clearly visible, especially in story drift ratios and plastic hinge

rotations. It is observed that IRSA is able to predict all nonlinear response quantities with a reasonable accuracy.

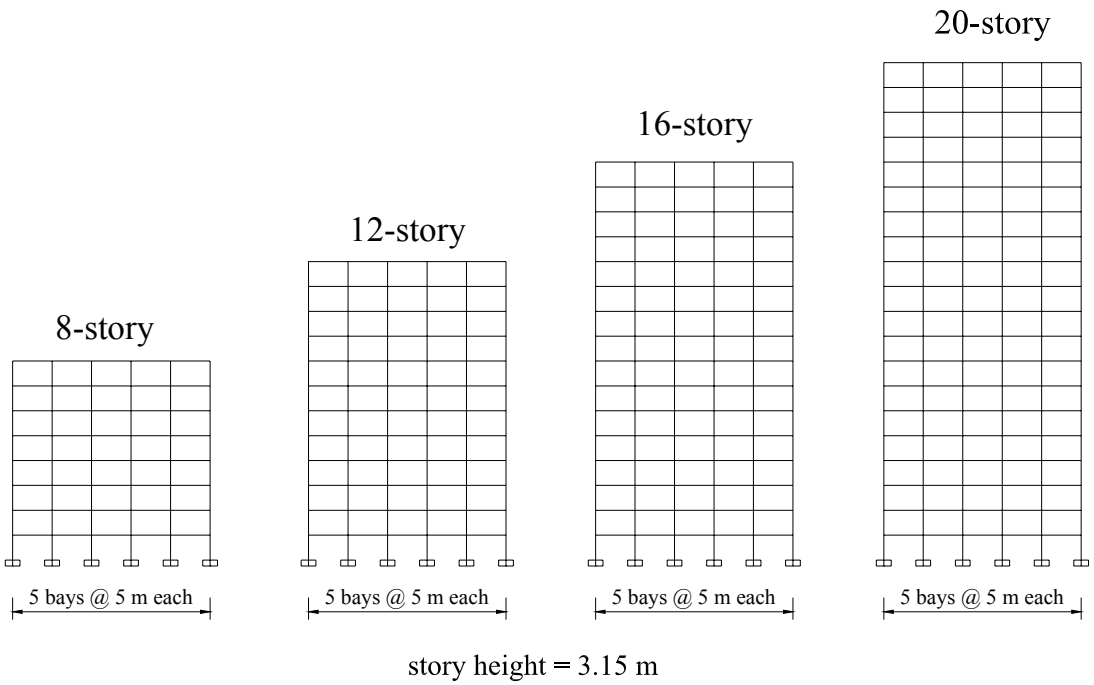

Fig. 6 Reinforced concrete frames considered in the parametric study

Table 1: Characteristics of Reinforced Concrete Frames

Number of Stories	Story	Side Columns (cm)	Internal Columns (cm)	Beam (cm)
8	1–5	45×45	50×50	30×60
	6–8	45×45	45×45	30×60
12	1–3	55×55	60×60	30×60
	4–12	55×55	55×55	30×60
16	1–3	60×70	60×70	30×60
	4–6	60×60	60×60	30×60
	7–9	60×50	60×50	30×60
	10–16	60×40	60×40	30×60
20	1–3	70×70	70×70	30×60
	4–6	60×70	60×70	30×60
	7–9	60×60	60×60	30×60
	10–12	60×50	60×50	30×60
	13–20	60×40	60×40	30×60

Table 2: Characteristics of Earthquake Records

No.	Earthquake	Mag.	Station	Dist. (km)	Site Cond.	PGA (*g*)	PGV (cm/s)	PGD (cm)
1	Chalfant Valley	6.2	54428 Zack Brothers Ranch	18.7	D	0.447	36.9	7.01
2	Chalfant Valley	6.2	54429 Zack Brothers Ranch	18.7	D	0.4	44.5	8.56
3	Loma Prieta, 1989	6.9	APEEL 2, Redwood City	47.9	D	0.22	34.3	6.87

4	Loma Prieta, 1989	6.9	1686 Fremont, Emerson Court	43.4	B	0.192	12.7	5.5
5	Mammoth Lakes, 1980	6	54214 Long Valley Dam	19.7	A	0.484	14.2	1.77
6	Mammoth Lakes, 1980	5.7	54214 Long Valley Dam	14.4	A	0.245	18.5	1.56
7	Mammoth Lakes, 1980	6	54301 Mammoth Lakes H.S.	14.2	D	0.39	23.9	2.72
8	Morgan Hill, 1984	6.2	47380 Gilroy Array #2	15.1	C	0.212	12.6	2.1
9	Morgan Hill, 1984	6.2	57382 Gilroy Array #4	12.8	C	0.348	17.4	3.11
10	Northridge. 1994	6.7	90074 La Habra, Briarcliff	61.6	C	0.206	12.3	1.23
11	Northridge, 1994	6.7	24575 Elizabeth Lake	37.2	C	0.155	7.3	2.7
12	Northridge, 1994	6.7	24611 LA—Temple	32.3	B	0.184	20	2.74
13	Northridge, 1994	6.7	90061 Big Tujunga, Los Angeles	24	B	0.245	12.7	1.12
14	Northridge, 1994	6.7	90021 LA—North Westmoreland	29	B	0.401	20.9	2.29
15	Whittier Narrows, 1987	6	Brea Dam (Downstream)	23.3	D	0.313	14.5	0.77
16	Whittier Narrows, 1987	6	108 Carbon Canyon Dam	26.8	A	0.221	8.7	0.64
17	Whittier Narrows, 1987	6	90034 LA—Fletcher Drive	14.4	C	0.213	12.6	1.45
18	Whittier Narrows, 1987	6	90063 Glendale—Las Palmas	19	C	0.296	17.1	1.82
19	Whittier Narrows, 1987	6	90021 LA—North Westmoreland	16.6	B	0.214	9.7	0.98
20	Whittier Narrows, 1987	6	24461 Alhambra, Fremont School	13.2	B	0.333	22	2.42

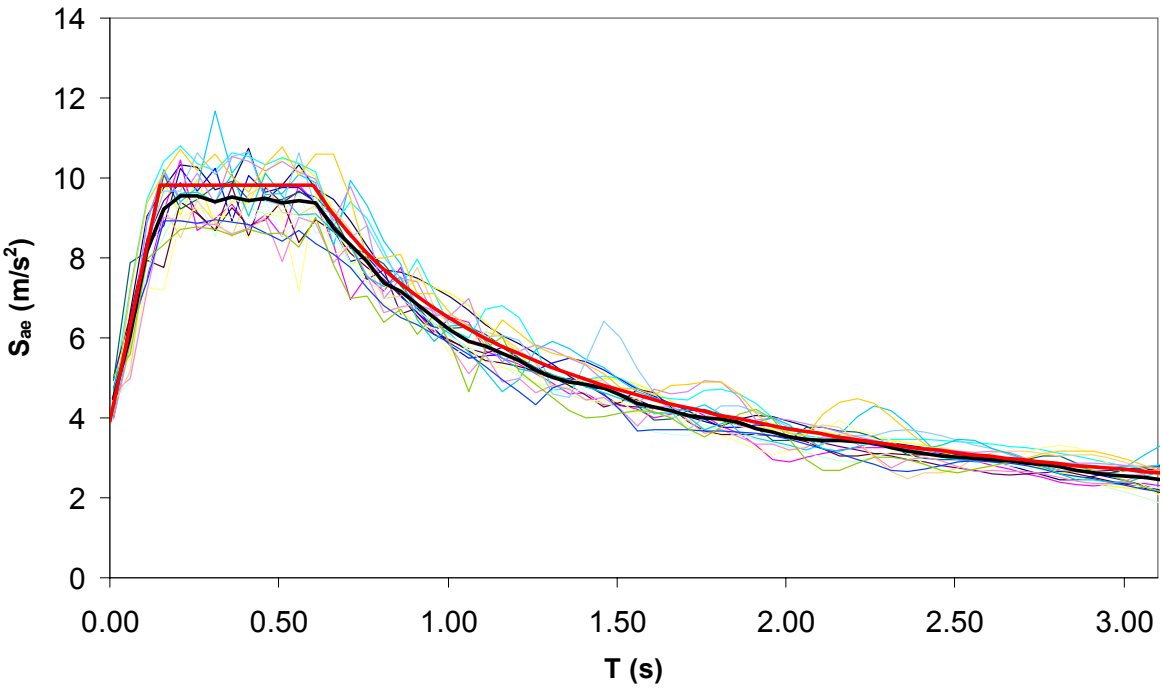

Fig. 7 Acceleration response spectra of the normalized records, and their mean superimposed on the code spectrum

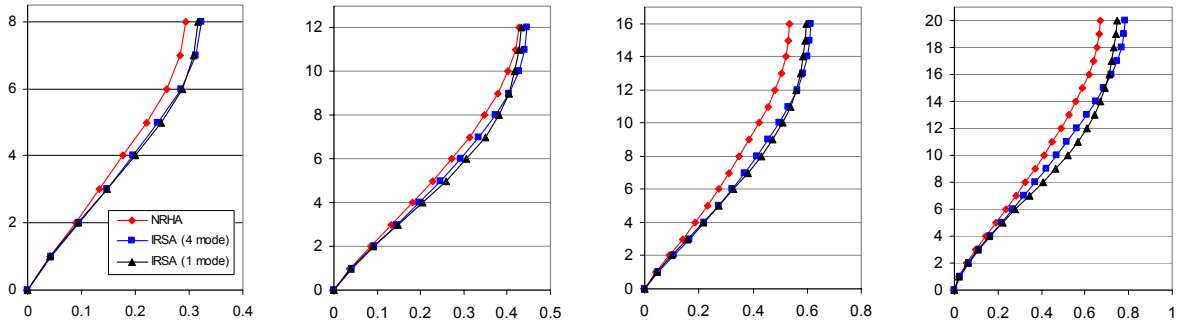

Fig. 8 Mean story displacements estimated by the nonlinear response history analysis (NRHA), four-mode IRSA, and single-mode IRSA for the 8-, 12-, 16- and 20-story frames

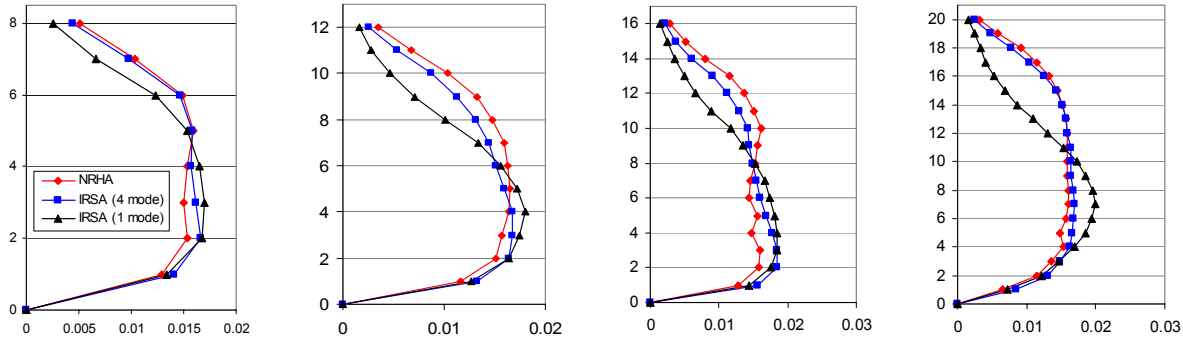

Fig. 9 Mean story drift ratios estimated by the nonlinear response history analysis (NRHA), four-mode IRSA, and single-mode IRSA for the 8-, 12-, 16- and 20-story frames

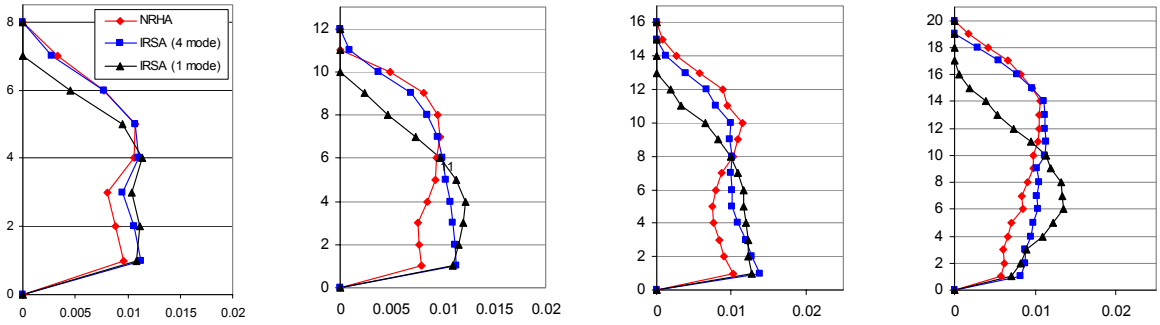

Fig. 10 Mean plastic rotations of central beams estimated by the nonlinear response history analysis (NRHA), four-mode IRSA, and single-mode IRSA for the 8-, 12-, 16- and 20-story frames

CONCLUSIONS

Incremental Response Spectrum Analysis (IRSA) procedure is presented as a direct extension of the linear Response Spectrum Analysis (RSA), which represents an improved multi-mode pushover analysis for performance-based nonlinear seismic assessment of existing buildings. The method is based on a piecewise linear approach, in which all linear operations are applicable in a piecewise linear pushover step in between the formation of consecutive plastic hinges. IRSA can be readily applied to any structure in practice where the earthquake input can be specified in the form of a smoothed response spectrum. To provide a clear and broader picture to the interested reader, in addition to the multi-mode analysis, single-mode pushover analyses with adaptive and invariant load patterns are also presented in detail.

As discussed in the introductory section of the paper, a clear distinction needs to be made between two types of pushover analysis, i.e., whether the analysis is performed for “capacity estimation” only or

whether it can be used as well for a "demand estimation" under a given earthquake ground motion. In this respect, attention was drawn to the fact that surprisingly a very small number of multi-mode pushover methods are available in the literature, which are capable of estimating the seismic demand.

Probably one of the most critical issues of almost all multi-mode pushover procedures is the "modal scaling", i.e., the assumption that has to be made for estimating the relative values of the modal displacement or modal pseudo-acceleration increments among various modes. In this respect, IRSA utilizes a novel approach based on scaling the modal displacements through instantaneous "inelastic spectral displacements". For practical applications this allows the direct use of linear response spectrum, thanks to the well-known "equal displacement rule". It was shown through a parametric study that IRSA is able to provide a reasonable accuracy for all nonlinear response quantities, including story drifts and plastic hinge rotations.

It should be stressed that all pushover procedures are approximate by nature and that none of them, including IRSA, can replace the rigorous nonlinear response history analysis, which is believed to prevail in the long run as a preferred engineering tool for seismic demand estimation. In the interim, pushover methods are expected to serve as practical nonlinear procedures, through which engineers will become acquainted with a realistic nonlinear seismic behavior of structures and which quantify the extent of structural damage, alas approximately, induced by a design earthquake. In this respect, it is believed that a practical pushover procedure must comply with the code practice, especially in specifying the seismic input in the form of a standard elastic response spectrum. This requirement is fully satisfied by IRSA. However it must be admitted that the application of IRSA is limited to the far-field earthquakes, as its fundamental assumption, i.e., equal displacement rule, is not applicable to the near-field earthquakes.

REFERENCES

1. Antoniou, S. and Pinho, R. (2004a). "Advantages and Limitations of Adaptive and Non-adaptive Force-Based Pushover Procedures", Journal of Earthquake Engineering, Vol. 8, No. 4, pp. 497–552.
2. Antoniou, S. and Pinho, R. (2004b). "Development and Verification of a Displacement-Based Adaptive Pushover Procedure", Journal of Earthquake Engineering, Vol. 8, No. 5, pp. 643–661.
3. Antoniou, S., Rovithakis, A. and Pinho, R. (2002). "Development and Verification of a Fully Adaptive Pushover Procedure", Proceedings of the 12th European Conference on Earthquake Engineering, London, U.K., Paper No. 822 (on CD).
4. ATC (1996). "Seismic Evaluation and Retrofit of Concrete Buildings: Volume 1", Report ATC-40, Applied Technology Council, Redwood City, California, U.S.A.
5. Aydınoğlu, M.N. (2003). "An Incremental Response Spectrum Analysis Based on Inelastic Spectral Displacements for Multi-Mode Seismic Performance Evaluation", Bulletin of Earthquake Engineering, Vol. 1, No. 1, pp. 3–36.
6. Aydınoğlu, M.N. (2004). "An Improved Pushover Procedure for Engineering Practice: Incremental Response Spectrum Analysis (IRSA)" in "Performance-Based Seismic Design Concepts and Implementation: Proceedings of an International Workshop, Bled, Slovenia, June 28–July 1, 2004 (edited by P. Fajfar and H. Krawinkler)", Report PEER 2004/05, University of California, Berkeley, U.S.A.
7. Aydınoğlu, M.N. (2005). "A Code Approach for Deformation-Based Seismic Performance Assessment of Reinforced Concrete Buildings", Proceedings of the International Workshop on Seismic Performance Assessment and Rehabilitation of Existing Buildings (SPEAR), Ispra, Italy, pp. 65–74.
8. Aydınoğlu, M.N. (2006). "Nonlinear Procedures in Revised Turkish Code for Seismic Performance Assessment and Retrofit Design", Proceedings of the First European Conference on Earthquake Engineering and Seismology, Geneva, Switzerland, Paper No. 450 (on CD).
9. Aydınoğlu, M.N. and Fahjan, Y.M. (2003). "A Unified Formulation of the Piecewise Exact Method for Inelastic Seismic Demand Analysis Including the P-Delta Effect", Earthquake Engineering & Structural Dynamics, Vol. 32, No. 6, pp. 871–890.
10. Aydınoğlu, M.N. and Kaçmaz, Ü. (2002). "Strength-Based Displacement Amplification Spectra for Inelastic Seismic Performance Evaluation", Report 2002/2, Kandilli Observatory and Earthquake Research Institute, Bogazici University, Istanbul, Turkey.

11. Bathe, K.J. (1996). "Finite Element Procedures", Prentice Hall, Upper Saddle River, U.S.A.
12. BSSC (1997). "NEHRP Guidelines for the Seismic Rehabilitation of Buildings (FEMA 273)", Report Prepared for the Federal Emergency Management Agency, Building Seismic Safety Council, National Institute of Building Sciences, Washington, DC, U.S.A.
13. CEN (2003). "Eurocode 8: Design of Structures for Earthquake Resistance—Part 1: General Rules, Seismic Actions and Rules for Buildings", prEN 1998-1 (Final Draft), Comité Européen de Normalisation, Brussels, Belgium.
14. Chopra, A.K. (2001). "Dynamics of Structures: Theory and Applications to Earthquake Engineering", Prentice Hall, Upper Saddle River, U.S.A.
15. Chopra, A.K. and Goel, R.K. (1999). "Capacity-Demand-Diagram Methods Based on Inelastic Design Spectrum", Earthquake Spectra, Vol. 15, No. 4, pp. 637–656.
16. Chopra, A.K. and Goel, R.K. (2002). "A Modal Pushover Analysis Procedure for Estimating Seismic Demands for Buildings", Earthquake Engineering & Structural Dynamics, Vol. 31, No. 3, pp. 561–582.
17. Elnashai, A.S. (2002). "Do We Really Need Inelastic Dynamic Analysis?", Journal of Earthquake Engineering, Vol. 6, No. 1 spec, pp. 123–130.
18. Fajfar, P. and Fischinger, M. (1988). "N-2-A Method for Nonlinear Seismic Analysis of Regular Structures", Proceedings of the Ninth World Conference on Earthquake Engineering, Tokyo-Kyoto, Japan, Vol. 5, pp. 111–116.
19. FEMA (2000). "Prestandard and Commentary for the Seismic Rehabilitation of Buildings", Report FEMA 356, Federal Emergency Management Agency, Washington, DC, U.S.A.
20. FEMA (2005). "Improvement of Nonlinear Static Seismic Analysis Procedures", Report FEMA 440, Federal Emergency Management Agency, Washington, DC, U.S.A.
21. Freeman, S.A., Nicoletti, J.P. and Tyrell, J.V. (1975). "Evaluations of Existing Buildings for Seismic Risk—A Case Study of Puget Sound Naval Shipyard, Bremerton, Washington", Proceedings of U.S. National Conference on Earthquake Engineering, Seattle, U.S.A., pp. 113–122.
22. Goel, R.K. and Chopra, A.K. (2004). "Evaluation of Modal and FEMA Pushover Analyses: SAC Buildings", Earthquake Spectra, Vol. 20, No. 1, pp. 225–254.
23. Goel, R.K. and Chopra, A.K. (2005). "Extension of Modal Pushover Analysis to Compute Member Forces", Earthquake Spectra, Vol. 21, No. 1, pp. 125–139.
24. Gupta, B. and Kunnath, S.K. (2000). "Adaptive Spectra-Based Pushover Procedure for Seismic Evaluation of Structures", Earthquake Spectra, Vol. 16, No. 2, pp. 367–391.
25. Hernandez-Montes, E., Kwon, O.-S. and Aschheim, M.A. (2004). "An Energy-Based Formulation for First- and Multiple-Mode Nonlinear Static (Pushover) Analyses", Journal of Earthquake Engineering, Vol. 8, No. 1, pp. 69–88.
26. Kalkan, E. and Kunnath, S.K. (2004). "Method of Modal Combinations for Pushover Analysis of Buildings", Proceedings of the 13th World Conference on Earthquake Engineering, Vancouver, Canada, Paper No. 2713 (on CD).
27. Kalkan, E. and Kunnath, S.K. (2006). "Adaptive Modal Combination Procedure for Nonlinear Static Analysis of Building Structures", Journal of Structural Engineering, ASCE, Vol. 132, No. 11, pp. 1721–1731.
28. McGuire, W., Gallagher, R.H. and Ziemian, R.D. (2000). "Matrix Structural Analysis", John Wiley & Sons, New York, U.S.A.
29. Miranda, E. and Akkar, S.D. (2003). "Dynamic Instability of Simple Structural Systems", Journal of Structural Engineering, ASCE, Vol. 129, No. 12, pp. 1722–1726.
30. MPWS (2006). "Specification for Buildings to be Built in Earthquake Zones", Ministry of Public Works and Settlement, Turkish Government, Ankara, Turkey (in Turkish).
31. Önem, G. (2006). "Spectral Displacement Amplification Factors for Higher Mode Capacity Diagrams with Steeper Post-Yield Slopes", Unpublished Report, Kandilli Observatory and Earthquake Research Institute, Bogazici University, Istanbul, Turkey.

32. Önem, G. and Aydınoğlu, M. (2006). "Verification of Improved Pushover Procedure IRSA (Incremental Response Spectrum Analysis)", Proceedings of the First European Conference on Earthquake Engineering and Seismology, Geneva, Switzerland, Paper No. 452 (on CD).
33. Paret, T.F., Sasaki, K.K., Eilbeck, D.H. and Freeman, S.A. (1996). "Approximate Inelastic Procedures to Identify Failure Mechanisms from Higher Mode Effects", Proceedings of the 11th World Conference on Earthquake Engineering, Acapulco, Mexico, Paper No. 966 (on CD).
34. Sasaki, K.K., Freeman, S.A. and Paret, T.F. (1998). "Multi-Mode Pushover Procedure (MMP)—A Method to Identify the Effects of Higher Modes in a Pushover Analysis", Proceedings of the Sixth U.S. National Conference on Earthquake Engineering, Seattle, U.S.A., Paper No. 271 (on CD).